Research Article | Vol. 27, No. 9 | 29 Apr 2019 | OPTICS EXPRESS 13182
Optics EXPRESS

Modal decomposition of Laguerre Gaussian beams with different radial orders using optical correlation technique

SRINIVAS PACHAVA, AWAKASH DIXIT, AND B. SRINIVASAN*

Department of Electrical Engineering, Indian Institute of Technology Madras, Chennai 600036, India
**balajis@ee.iitm.ac.in*

Abstract: In this paper, we explore the use of an optical correlation technique to decompose different radial as well as azimuthal order modes of Laguerre Gaussian (LG) beams. We experimentally demonstrate the decomposition of single as well as composite LG beams and compare it with simulations. We report the modal decomposition with 27 dB extinction over several radial and azimuthal orders. Finally, we show that our modal decomposition is capable of sorting mode spectrum consisting of up to 10 LG modes with an accuracy of better than 97.8%.

1. Introduction

In quantum information processing and quantum key distribution (QKD), increased number of quantum states could provide faster data manipulation with enhanced security [1]. Specifically, an increase in the number of orthogonal states in a quantum communication link could potentially improve both its security and photon efficiency. Such orthogonality in optical beams has also been exploited in classical communication channels to increase the data rates, for example Tb/s data rates have been demonstrated in both free-space [2] and optical fiber links [3,4].

Laguerre Gaussian (LG) beams with different radial and azimuthal modal numbers are a family of orthogonal basis set that has been gaining widespread attention lately. In particular, LG beams with different azimuthal modal number (the so-called "vortex" beams) are widely exploited in the optical communications [2–4]. Recently, it has been argued that radial modal number should also be used to increase the space-bandwidth product [5] of an optical system.

One of the key issues in tracking the propagation of such beams as well as their demodulation is the quantification of their purity. To accomplish this, we need robust mode sorters or modal decomposition algorithms that accommodate a wide range of the modal spectrum with high accuracy. Recently, Guodong *et al*. experimentally demonstrated a 200 Gbit/s free-space optical link with a bit error rate of 3.8×10^{-3} by multiplexing LG beams with different radial indices [6]. In such experiments, they clearly show that the bit error rate primarily depends on the mode demultiplexing or decomposition method at the receiver end.

While excellent results have been demonstrated with practical mode sorters [7,8], they have been limited in the number of modes that they can sort. On the other hand, modal decomposition has been demonstrated to address a wide range of the spectrum although their accuracy may be limited by the specific algorithm that is used [9–11]. For example, the same group mentioned above has reported 15 dB power extinction between the zeroth and first radial order LG modes using an optical correlation technique at the receiver end [12]. This is limited by the fact that they have used only the phase structure of the LG modes in the decomposition process.

In this work, we demonstrate the use of an optical correlation technique that incorporates both amplitude as well as phase structure of LG modes to accomplish the modal decomposition. We experimentally demonstrate >25 dB power extinction between zeroth and

#358570 https://doi.org/10.1364/OE.27.013182
Journal © 2019 Received 25 Jan 2019; revised 5 Apr 2019; accepted 5 Apr 2019; published 25 Apr 2019

Optics EXPRESS

first radial order LG modes, limited only by the bit resolution of the camera used in our setup. We have also verified the decomposition of composite, mode-multiplexed beams consisting of up to 10 different radial/azimuthal modes. Finally, we show that we can potentially extend this technique to measure the power of Bessel beams with higher radial orders [13] in optical fiber by properly considering the polarization into account [14].

2. Modal decomposition based on optical correlation technique

Modal decomposition is a well-known technique for analyzing the structure of an optical beam upon propagation and has been widely used for several different applications. For example, modal decomposition based on optical correlation technique has been used to determine the beam quality upon propagation in a few-mode optical fiber [15]. It has also been used to determine the angular momentum density of Bessel beams [11] and recently, the technique has been used by Andrew et al. for analyzing an image transmitted through a turbulent medium [10,16]. In our article, we use a similar technique for decomposing the mode multiplexed LG beams with different radial and azimuthal orders. Specifically, we perform modal decomposition based on computer-generated holograms (CGHs) using spatial light modulator (SLM) as described below.

The transverse electric field of a linearly polarized LG beam in cylindrical coordinates (ρ,ϕ) is given by the expression,

$$LG_{l,p} = C_{l,p}\exp\left(\frac{-\rho^2}{w^2}\right)\left(\frac{\sqrt{2}\rho}{w}\right)^{|l|} LG_p^{|l|}\left(\frac{2\rho^2}{w^2}\right)\exp(il\phi), \tag{1}$$

where w is the beam waist, $C_{l,p}$ is a constant, $LG_p^{|l|}$ is a generalized Laguerre polynomial with azimuthal and radial indices of l and p respectively. The constants $C_{l,p}$ is chosen such that the LG beams form an orthonormal basis set. Here we consider only horizontally polarized beams as our SLM responds to only that polarization state.

In modal decomposition method, any scalar light beam (U) can be represented by a superposition of $LG_{l,p}$ modes with corresponding complex weights $W_{l,p}$ as shown in Eq. (1). The complex weight of a mode is calculated by optically correlating the input beam with the complex conjugate of the mode (Eq. (3)).

$$U = \sum\nolimits_{l,p} W_{l,p} LG_{l,p} \tag{2}$$

$$W_{l,p} = \iint U LG_{l,p}^{*} r dr d\phi \tag{3}$$

Equation (3) is essentially a dot product operation between the input beam and the complex conjugate of the mode. To perform this operation experimentally, we use a spatial light modulator (SLM) and convex lens as shown in Fig. 1. The input beam $LG_{l,p}$ is multiplied with its complex conjugate mode using a SLM by encoding necessary holograms (discussed below). To perform the integral operation, we propagate the reflected beam through the convex lens.

Optics EXPRESS

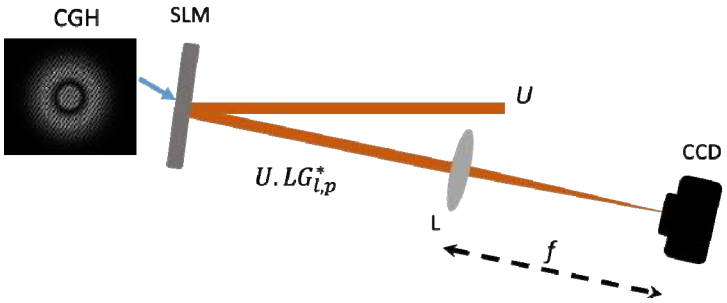

Fig. 1. Experimental realization of dot product operation.

The electric field corresponding to the reflected beam at the Fourier plane of the convex lens is given by Eq. (4) [17].

$$U_f(u,v) = \frac{\exp(ikf)\exp\left(\frac{ikr^2}{2f}\right)}{i\lambda f}\int_{-\infty}^{\infty}\int ULG^{*}_{l,p}\exp\left(-\frac{i2\pi\rho r}{\lambda f}\cos(\Theta-\phi)\right)\rho d\rho d\phi, \quad (4)$$

where $r = \sqrt{(u^2+v^2)}$, $\Theta = \tan^{-1}(u/v)$, *u and v* are spatial frequencies, *f* is the focal length of the convex lens, λ is the wavelength, and *k* is the propagation constant of the beam.

The center of the Fourier plane $U_f(0,0)$, which is commonly referred as the DC component gives the weight of the $LG_{l,p}$ mode. Since the camera captures the intensity, we take the square root of the observed intensity to obtain the field weight. However, it should be noted that we lose the phase information of the beam in this process and as such, we do not capture the relative phase between different modes.

By following the above procedure, the complex weight $W_{l,p}$ of different modes may be determined by loading the de-multiplexing hologram of each mode on the SLM. A key aspect of our technique is the utilization of both the phase and amplitude structure of the target LG mode for optical correlation. Previously, different methods have been proposed by Davis et al [18], Long et al [19], and Arrizon et al [20] for generating the scalar field from the phase-only SLM. Of these, Arrizon's algorithm is widely used because it has been demonstrated to provide relatively high signal to noise ratio [21] and it requires <1.17π phase range of the SLM.

In this approach, any complex field *s(x,y)* with amplitude function *a(x,y)* ranging from 0 to 1 and phase function *θ(x,y)* as expressed in Eq. (5) can be generated through the CGH using a phase modulation function $\Psi(a,\theta)$ represented in Eq. (6).

$$s(x,y) = a(x,y)\exp(i\theta(x,y)) \quad (5)$$

$$\Psi(a,\theta) = f(a)\sin(\theta), \quad (6)$$

where *f(a)* has to be accurately determined to generate the complex field. This process is explained below.

When a beam with electric field *U* is incident on the SLM encoded with such phase modulation function $\Psi(a,\theta)$, the beam is spatially modulated. The reflected beam from the SLM can be expressed in Fourier series expansion using Jacobi–Anger identity [22] as,

$$U\exp(if(a)\sin(\theta)) = U\sum_{-\infty}^{\infty} J_m[f(a)]\exp(im\theta), \quad (7)$$

Optics EXPRESS

where J_m is the Bessel function of first kind with order m. In the Fourier expansion, the phase of the first component (m = 1) is identical to the phase structure of the complex field. Also, by equating the magnitude of the first component to the magnitude function of the complex field as shown in Eq. (8), f(a) can be determined.

$$f(a) = J_1^{-1}[Aa], \tag{8}$$

where A is a constant.

The maximum value of A for which Eq. (8) can be satisfied is $A \cong 0.5819$, which corresponds to the first maximum of the first-order Bessel function J_1. Since the corresponding argument of the first order Bessel function is 1.84, the required phase range of the SLM in this case is $-1.17\pi/2$ to $+ 1.17\pi/2$. Hence by substituting Eq. (8) in Eq. (7), we generate complex function $s(x,y)$ in the first harmonic of the above Bessel series. In order to achieve the spatial isolation of $s(x,y)$ from the other harmonics, a phase carrier $2\pi(u_0 x + v_0 y)$ is added to the phase of the encoded field, θ (Eq. (9)).

$$U\exp\left(if(a)\sin\left(\theta + 2\pi\left(u_0 x + v_0 y\right)\right)\right) = U\sum_{-\infty}^{\infty} J_m\left[f(a)\right]\exp\left(im\left(\theta + 2\pi\left(u_0 x + v_0 y\right)\right)\right) \tag{9}$$

The resultant first order diffraction from the SLM (Eq. (10)) is propagated through lens to accomplish the dot product operation.

$$U.a(x,y)\exp\left(i\theta(x,y) + 2\pi\left(u_0 x + v_0 y\right)\right) \tag{10}$$

It is to be noted that the higher order Fourier components in the image plane consist of weights of higher azimuthal charges of the incident LG beam, which may be useful for sorting the modes of composite beams. However, in our work, we consider only the first order Fourier component and sequentially sort multiple modes in the same setup.

3. Experimental details

Based on the above optical correlation algorithm, we proceed to experimentally demonstrate the modal decomposition of azimuthal as well as radial orders of LG beams. The schematic of the experimental setup used to implement the optical correlation technique is shown in Fig. 2(a).

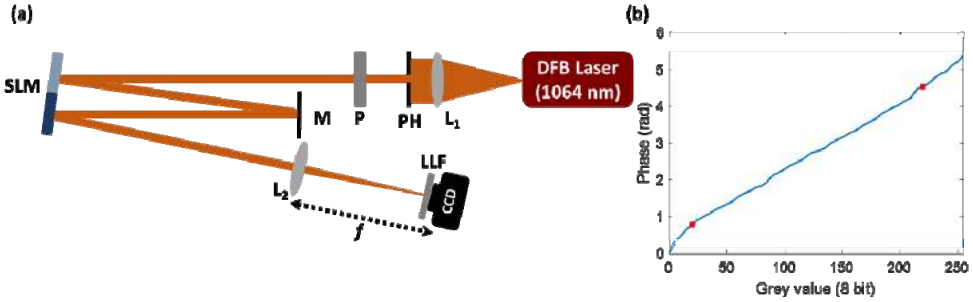

Fig. 2. (a) Experimental setup for implementing the optical correlation technique. DFB: Distributed feedback laser; L_1 (f = 10 cm), L_2 (f = 20 cm): Convex lens; PH: Pin-hole; P: Polarizer; SLM: Spatial light modulator; M: mirror; LLF: Laser line filter at 1064 nm; CCD: Charge-coupled device camera. (b) Phase response of the SLM at 1064 nm wavelength.

The output beam from a polarization maintaining fiber-pigtailed distributed feedback (DFB) laser source (Lumics, Inc.) at 1064 nm wavelength is collimated using a convex lens (L_1, f = 10 cm). The collimated beam is transmitted through a polarizer (P) to ensure that we obtain a horizontally polarized beam aligned to the preferred polarization axis of the phase-only spatial light modulator (HoloEye PLUTO-2-NIRO-023). The phase response of the SLM is shown in Fig. 2(b). We use the linear portion (between the highlighted red spots) of 1.17π

Optics EXPRESS

radians for generating the holograms. In our experiments, the SLM is partitioned into two equal halves. One half is programmed to generate the required LG beam and the other half is programmed to perform the dot product operation as part of the modal decomposition.

A mirror (M) is used to direct the beam generated from one half of the SLM to the other half corresponding to a propagation distance of 30 cm. The diffracted beam from the second half of the SLM is collected using a convex lens (L_2 with f = 20 cm) located at a distance of 50 cm from the SLM and is imaged in the Fourier plane using a CCD camera (Thorlabs Inc.). A laser line filter is incorporated in front of the camera to filter the ambient light. As mentioned earlier, we observe the DC component in the Fourier plane to obtain the weight of a particular mode. By loading the appropriate CGH on the SLM, the modal weights of different modes are obtained.

4. Results and discussion

We initially implement the optical correlation algorithm for modes with different radial number (p = 0, 1) and same azimuthal number (l = 0), like LG_{00} and LG_{01} modes. The LG_{00} mode of beam waist 0.8 mm is generated by loading the appropriate CGH computed using the above Arrizon's algorithm [20] on the first half of the SLM (shown in Fig. 3(a)). The first order diffracted beam is then used for modal decomposition in the second half of the SLM by performing the dot product operation with decomposition CGHs corresponding to the LG_{00} and LG_{01} modes (shown in Figs. 3(c), and 3(d) respectively). Since the diffracted beam is typically larger than the above beam waist (0.8 mm), we need to vary the decomposition CGH radius (denoted as 'R' in Figs. 3(c), and 3(d)) to determine the optimum radius that provides the best extinction in the transmitted power between the target mode and its orthogonal mode. For example, when we generate a LG_{00} mode we anticipate maximum extinction between the target LG_{00} mode (matched) and the LG_{01} mode (orthogonal) for a particular radius of the decomposition CGH. The results from such an experiment are shown in Fig. 3(e), wherein the normalized power measured for different combination of generation and decomposition CGH settings is plotted as a function of different radius (R) of the decomposition CGH. Note that the normalization is performed with respect to the power measured in the desired mode.

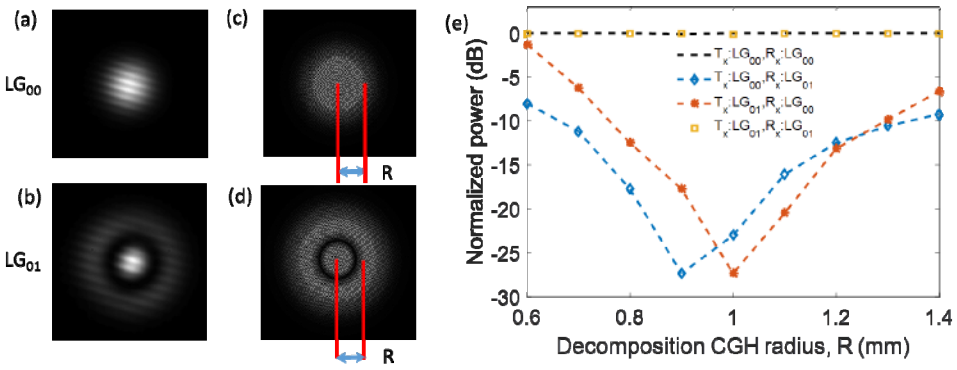

Fig. 3. (a), (b) Intensity patterns of LG_{00}, LG_{01} modes respectively. (c), (d) Decomposition CGHs of LG_{00} and LG_{01} modes respectively, R: decomposition CGH radius. (e) Normalized power measured for different combination of generation (T_x) and decomposition (R_x) CGH settings as a function of decomposition CGH radius.

From Fig. 3(e), we note that the maximum power extinction of ~27 dB is obtained between LG_{00} (matched) and LG_{01} (orthogonal) modes for a decomposition CGH radius of 0.9 mm when the generation CGH corresponds to the LG_{00} mode. A similar power extinction of 27 dB between the LG_{00} (orthogonal) and LG_{01} (matched) modes is observed when the

Optics EXPRESS

generation CGH corresponds to the LG_{01} mode (given in Fig. 3(b)). Interestingly, the maximum extinction in this case occurs for a decomposition CGH radius of 1 mm. We attribute the difference in the decomposition CGH radius to the spherical aberration of the SLM as well as the convex lens for a beam of higher order transverse mode such as the LG_{01} beam [23]. Note that the maximum extinction that could be measured in our experiments (27 dB) is limited by the bit depth of the camera used (8 bit) and it could be improved further by using a higher bit camera.

The Fourier plane images captured with the camera for the above matched and orthogonal cases are shown in Fig. 4. The first and second rows represent the Fourier plane images of LG_{00} beam optically correlated with LG_{00} (matched) and LG_{01} (orthogonal) modes respectively. When the LG_{00} decomposition CGH radius is increased, the DC component (center value of the Fourier plane) remains constant. Whereas the DC component corresponding to the orthogonal mode (LG_{01}) gradually decreases, reaches minimum at 0.9 mm decomposition CGH radius and then increases. Similarly, the Fourier plane images obtained by optically correlating LG_{01} beam with LG_{00} (orthogonal) and LG_{01} (matched) modes are shown in third and fourth rows of Fig. 4 respectively. When the LG_{00} decomposition CGH radius is increased, the DC component (center value of the Fourier plane) gradually decreases, reaches minimum at 1.0 mm waist and then increases. Please note that these results are quantified through the plot of Fig. 3(e), as discussed above.

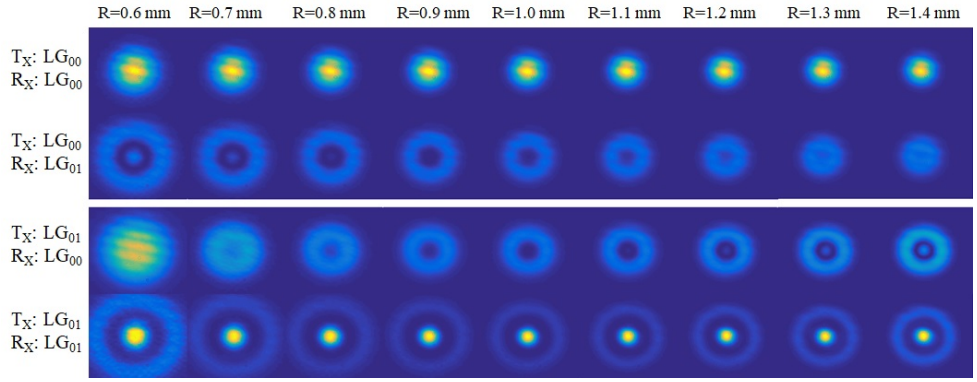

Fig. 4. First and second rows - Fourier plane images obtained by optically correlating LG_{00} beam with LG_{00} (matched) and LG_{01} (orthogonal) modes; Third and fourth rows - LG_{01} beam with LG_{00} (orthogonal) and LG_{01} (matched) modes.

We extend the implementation of our optical correlation algorithm for modes with different radial number (p = 0, 1) and higher azimuthal number (l = 1), specifically the LG_{10} (Fig. 5(a)), and LG_{11} (Fig. 5(b)) modes. The decomposition CGHs corresponding to LG_{10}, LG_{11} modes are shown in Figs. 5(c), and 5(d) respectively. As described earlier, the decomposition CGH radius of LG_{10} and LG_{11} modes are varied and the measured power values for the matched and orthogonal cases are shown in Fig. 5(e). A power extinction of 27 dB is obtained at 0.9 mm and 1.0 mm, between the LG_{10} and LG_{11} modes when the generation CGH corresponds to LG_{10} and LG_{11} modes, respectively (orthogonal cases). The Fourier plane images associated to these measurements are shown in Fig. 6, which are quantified in the plot of Fig. 5(e).

Optics EXPRESS

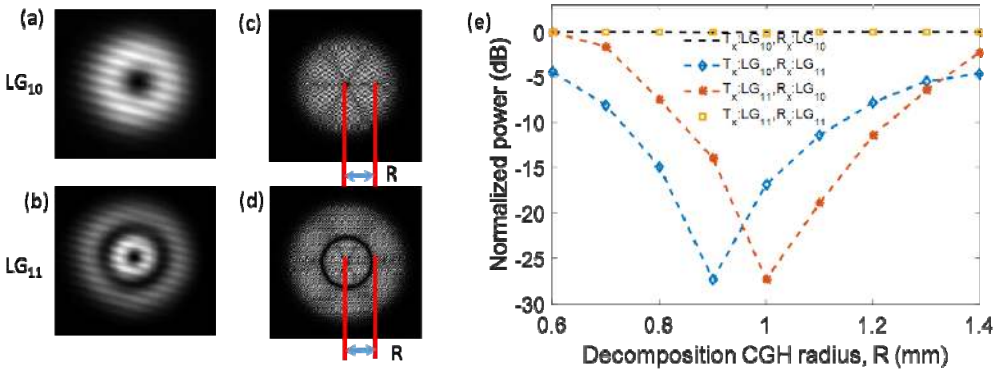

Fig. 5. (a), (b) Intensity patterns of LG_{10}, LG_{11} modes respectively. (c), (d) Decomposition CGHs of LG_{10} and LG_{11} modes respectively, R: decomposition CGH radius. (e) Normalized power measured for different combination of generation (T_x) and decomposition (R_x) CGH settings as a function of decomposition CGH radius.

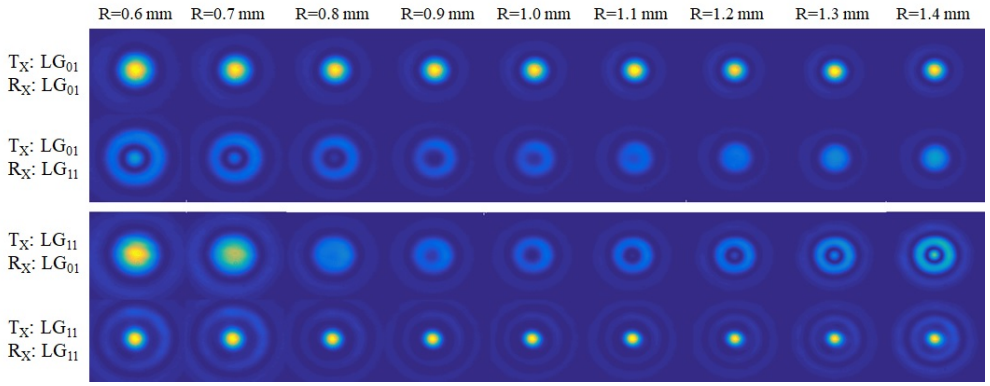

Fig. 6. First and second rows - Fourier plane images obtained by optically correlating LG_{10} beam with LG_{10} (matched) and LG_{11} (orthogonal) modes; Third and fourth rows – LG_{11} beam with LG_{10} (orthogonal) and LG_{11} (matched) modes.

In the above experiments, we prove that we can achieve high extinction (27 dB, limited by the camera bit resolution) between the matched and orthogonal cases when we use two radial order modes (p = 0, 1) with two azimuthal order modes (l = 0, 1). It remains to be seen whether this technique is scalable to higher mode indices. In order to explore this, we extended the above optical correlation experiments to higher azimuthal order modes (l = –4 to + 4). The observations from such experiments are summarized using a parity plot (Fig. 7). For simplicity, we used a constant decomposition CGH radius R of 1.0 mm for these experiments.

Optics EXPRESS

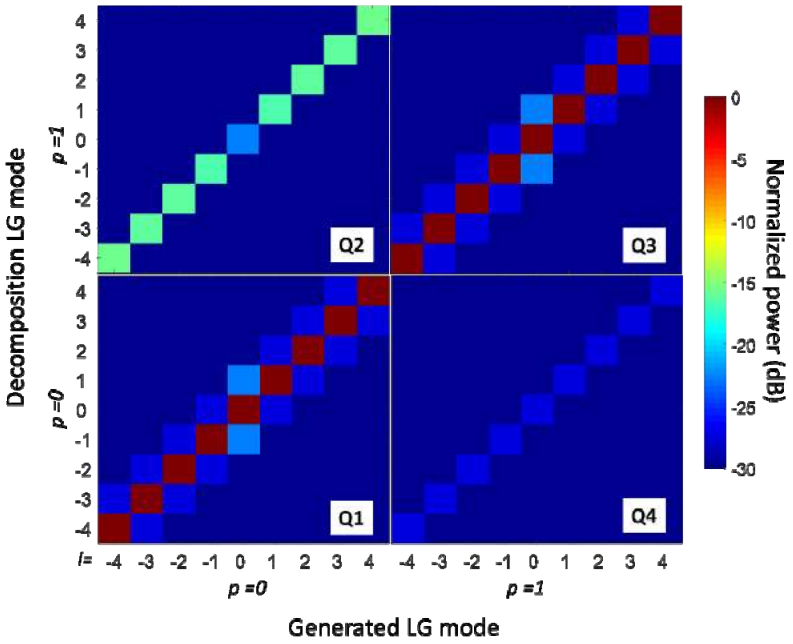

Fig. 7. Normalized power measured from optical correlation technique for different combinations of generated and decomposition LG modes with radial mode order p = 0, 1 and azimuthal mode order l = –4 to + 4. Diagonal elements represent parity and the off-diagonal elements represent the magnitude of coupling to neighboring modes. Q1-Q4 corresponds to the different quadrants in the above plot.

The diagonal elements of the parity plot represent the power measured when the generated and decomposition CGH corresponding to LG modes are matched and the off-diagonal elements represent the power coupled to neighboring modes. From Fig. 7, we observe the following: when LG beams with p = 0 and l = –4 to + 4 are generated and correlated with matched decomposition CGH patterns (corresponding to diagonal values in Q1 quadrant), the normalized power is uniform and maximum. However, we do observe a finite amount of power when correlated with the orthogonal p = 1 decomposition CGH patterns (corresponding to diagonal values in Q2). For l = 0 mode, we observe an extinction of ~23dB. This degradation of extinction compared to an expected value of 27 dB is due to the non-optimal decomposition CGH radius of 1 mm used in the above measurements (as evident from Fig. 3(e)). Furthermore, we observe an increase in the power measured as we increase the azimuthal number (l). For example, when LG_{-40} is generated, we noticed only 15.5 dB extinction between LG_{-40} and LG_{-41} modes. This degradation in extinction for higher order azimuthal modes is once again attributed to the wavefront aberration introduced by the SLM as well as the associated optics for a beam of higher order transverse mode such as the LG beams studied here [23].

Interestingly, when LG beams with p = 1 are generated we noticed that power coupling to the p = 0 LG modes is much lower (extinction of 27 dB, corresponding to diagonal values in Q4). Specifically, when LG_{-41} is generated we obtained 27 dB extinction between LG_{-41} and LG_{-40} modes (which is better than the converse case). This is not surprising since we are using the optimal decomposition CGH radius for this case compared to the above case.

It should be noted that a similar optical correlation technique has been reported recently by other groups. A collinear phase shifting holographic method [24] is reported with a modal extinction ratio of ~24 dB between $LG_{1,0}$ and $LG_{1,1}$. Another optical correlation technique based on phase retrieval method [25] is reported for decomposing $LG_{l,p}$ (l = 0, $0 \le p \le 2$)

Optics EXPRESS

modes with less than 10 dB modal extinction ratio between the mode of interest and the neighbouring modes. Optical correlation technique based on intensity flattening [26] is reported for decomposing $LG_{l,p}$ ($l = 0$, $0 \le p \le 7$) radial order modes. Unfortunately, modal extinction ratios of the decomposed modes are not presented in the article. A maximum visibility (ratio of the power in the desired mode to the power in all the modes) of 99.1% is reported. Finally, a radial mode sorter [27] has been reported for decomposing $LG_{l,p}$ ($-2 \le l \le 2$, $0 \le p \le 1$) modes with a maximum modal extinction ratio of 10 dB.

In comparison with the above methods, our method is tested for $LG_{l,p}$ ($-4 \le l \le 4$, $0 \le p \le 1$) modes having both azimuthal and radial orders. We obtain a modal extinction ratio of 27 dB (limited by our camera resolution) irrespective of the input mode, which is greater than any of the extinction ratios of the above mentioned schemes. We obtain a visibility of ~99.9% in our experiments, which is also greater than the visibility obtained in optical correlation technique based on intensity flattening [26].

So far, we discussed the modal decomposition using optical correlation algorithm for the case wherein only a single mode is generated. In several practical applications including Mode Division Multiplexing systems, modal decomposition has to be performed for composite (two or more) modes. In the following discussion, we demonstrate the use of the optical correlation algorithm to perform modal decomposition for (i) the case of two generated LG modes followed by (ii) the case of 10 generated LG modes.

For the first case, we generate a composite beam consisting of LG_{00}, LG_{01} modes for several relative power levels. We decompose the individual modes using the appropriate decomposition CGHs (Figs. 3(c), and 3(d)) for a decomposition CGH radius of $R = 1.0$ mm and finally obtained the relative power levels of the decomposed modes. The parity plot of the relative power levels for decomposed modes versus that for generated modes is shown in Fig. 8(a).

From Fig. 8(a), we notice that the negative ratio values for the generated modes (power in LG_{00} mode < power in LG_{01}) yield the expected ratio values for the decomposed modes within experimental error bars. On the other hand, we observe a deviation from the ideal parity line for positive ratio values for the generated modes (power in LG_{00} mode > power in LG_{01}). For example, a 10 dB power deviation (well beyond our experimental error) is observed between them when the generated LG_{00} mode power is 24 dB higher than the LG_{01} mode power. We notice a similar behavior when we consider a composite beam with LG_{10} and LG_{11} modes.

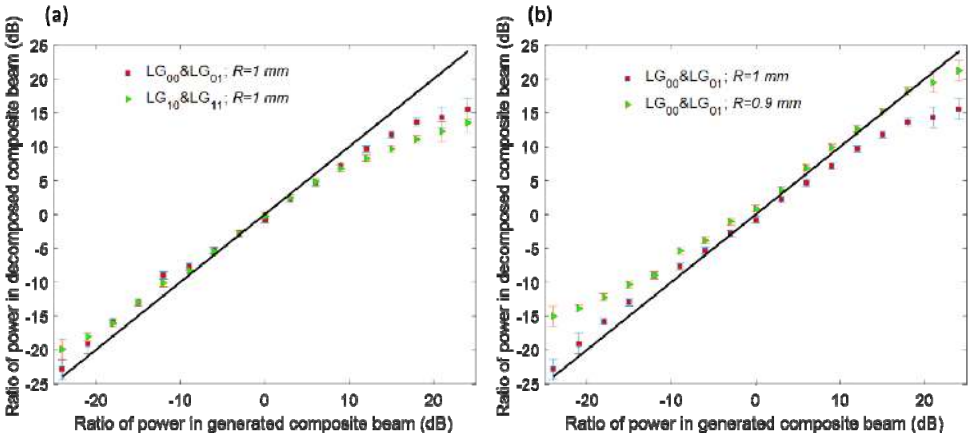

Fig. 8. (a) Decomposition power extinction Vs. generated power extinction of composite beams LG_{00} and LG_{01}, LG_{10} and LG_{11} for $R = 1$ mm. (b) Decomposition power extinction Vs. generated power extinction of LG_{00} and LG_{01} composite beam for $R = 1$ mm and $R = 0.9$ mm.

Optics EXPRESS

One possible explanation for the above behavior is the variance in the decomposition CGH radius for the LG_{00} and LG_{01} modes as demonstrated in Fig. 3(e). In order to verify this hypothesis, we performed the optical correlation of composite (LG_{00}, LG_{01}) mode at a decomposition CGH radius of 0.9 mm as well. The ratio value of decomposition power for different ratio values of generated power for R = 1.0 mm and R = 0.9 mm are shown in Fig. 8(b). In case of R = 0.9 mm, the decomposition ratio values are consistent with that for generated modes for positive ratio values, whereas for negative ratio values, they deviate from the parity line. This behavior is exactly opposite to the R = 1.0 mm case, which confirms the above hypothesis.

Finally, we demonstrate the use of the optical correlation algorithm for decomposing a composite beam consisting of LG_{-21} and LG_{21} modes the results of which are shown in Fig. 9. The decomposition is carried out for radial modal indices p = 0, 1 as well as azimuthal modal indices l = –4 to + 4.

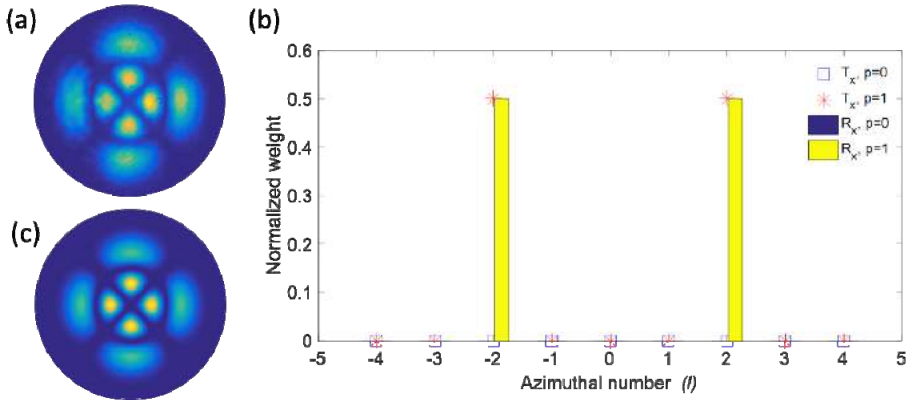

Fig. 9. (a) Intensity structure of the generated composite beam consisting of LG_{-21} and LG_{21} modes. (b) Weights of the generated (markers) and decomposition (bars) LG mode spectrum for radial orders p = 0, 1 plotted as a function of different azimuthal mode indices l = –4 to + 4. (c) Intensity structure simulated using the experimentally obtained modal weights.

As seen in Fig. 9(b), we observe an excellent match between the weights of the generated composite beam and the decomposed composite beam. Moreover, the extinction for the other modes is found to be 27 dB (although not obvious in Fig. 9(b)) thereby reconfirming the results presented earlier in Fig. 7. We show further that the intensity structure of the reconstructed composite beam based on the decomposed beam weights illustrated in Fig. 9(c) closely resembles the generated intensity structure of Fig. 9(a).

We extended the above investigation to the case of a composite beam consisting of 10 different LG modes (azimuthal mode indices l = –2 to + 2 and radial mode indices p = 0, 1). A sample modal distribution is chosen such that the generated mode weights (denoted as markers in Fig. 10) are halved for consecutive azimuthal mode index (both positive and negative values). As in the above case, we observe that the decomposed modal weights agree well with the generated modal weights across the entire mode spectrum. The relatively high error observed for the LG_{-20} and LG_{20} modes are due to the non-optimal radius of the decomposition CGH, as explained previously. However, the intensity structure of the reconstructed beam (illustrated in Fig. 10(c)) based on the experimentally obtained modal weights closely resembles the generated composite beam of Fig. 10(a).

Optics EXPRESS

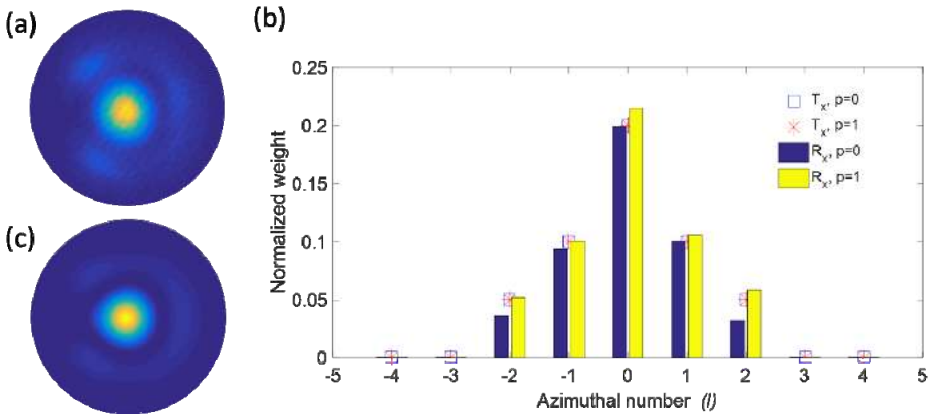

Fig. 10. (a) Intensity structure of the generated composite beam consisting of 10 LG modes. (b) Weights of the generated (markers) and decomposition (bars) LG mode spectrum for radial orders p = 0, 1 plotted as a function of different azimuthal mode indices l = –4 to + 4. (c) Intensity structure simulated using the experimentally obtained modal weights.

5. Conclusions

In conclusion, we report the first systematic study on the decomposition of LG modes consisting of different radial order as well as azimuthal modes using the optical correlation technique. We demonstrate high extinction (27 dB) while decomposing the LG beam irrespective of the modal index, although it requires a slight adjustment of the decomposition CGH radius. This result is well supported through a parity plot consisting of radial modal index p = 0, 1 as well as azimuthal modal index l = –4 to + 4. We also demonstrate strong decomposition performance for the case of composite beam consisting of two LG beams with better than 93% accuracy over a dynamic range of 20 dB, limited by the above adjustment of the decomposition CGH radius. The modal decomposition has been extended to a composite mode spectrum consisting of 10 modes, with an accuracy of better than 97.8%. Efforts are underway to realize the potential of the optical correlation technique demonstrated here to perform a single shot decomposition of composite LG beams.

Funding

Asian Office of Aerospace Research and Development (AOARD) (FA2386-16-1-4077); Ministry of Human Resources & Development (MHRD, Government of India)

Acknowledgments

The authors would like to acknowledge Shanti Bhattacharya, IIT Madras for lending components, and Siddharth Ramachandran, Boston University for technical discussions.

References

1. A. Mair, A. Vaziri, G. Weihs, and A. Zeilinger, "Entanglement of the orbital angular momentum states of photons," Nature **412**(6844), 313–316 (2001).
2. J. Wang, J. Y. Yang, I. M. Fazal, N. Ahmed, Y. Yan, H. Huang, Y. Ren, Y. Yue, S. Dolinar, M. Tur, and A. E. Willner, "Terabit free-space data transmission employing orbital angular momentum multiplexing," Nat. Photonics **6**(7), 488–496 (2012).
3. G. Zhu, Z. Hu, X. Wu, C. Du, W. Luo, Y. Chen, X. Cai, J. Liu, J. Zhu, and S. Yu, "Scalable mode division multiplexed transmission over a 10-km ring-core fiber using high-order orbital angular momentum modes," Opt. Express **26**(2), 594–604 (2018).
4. L. Zhu, G. Zhu, A. Wang, L. Wang, J. Ai, S. Chen, C. Du, J. Liu, S. Yu, and J. Wang, "18 km low-crosstalk OAM + WDM transmission with 224 individual channels enabled by a ring-core fiber with large high-order mode group separation," Opt. Lett. **43**(8), 1890–1893 (2018).
5. A. W. Lohmann, R. G. Dorsch, D. Mendlovic, C. Ferreira, and Z. Zalevsky, "Space–bandwidth product of optical signals and systems," J. Opt. Soc. Am. A **13**(3), 470–473 (1996).

Optics EXPRESS

6. G. Xie, Y. Ren, Y. Yan, H. Huang, N. Ahmed, L. Li, Z. Zhao, C. Bao, M. Tur, S. Ashrafi, and A. E. Willner, "Experimental demonstration of a 200-Gbit/s free-space optical link by multiplexing Laguerre-Gaussian beams with different radial indices," Opt. Lett. **41**(15), 3447–3450 (2016).
7. G. C. G. Berkhout, M. P. J. Lavery, J. Courtial, M. W. Beijersbergen, and M. J. Padgett, "Efficient sorting of orbital angular momentum states of light," Phys. Rev. Lett. **105**(15), 153601 (2010).
8. S. Lightman, G. Hurvitz, R. Gvishi, and A. Arie, "Miniature wide-spectrum mode sorter for vortex beams produced by 3D laser printing," Optica **4**(6), 605–610 (2017).
9. M. Lyu, Z. Lin, G. Li, and G. Situ, "Fast modal decomposition for optical fibers using digital holography," Sci. Rep. **7**(1), 6556 (2017).
10. A. Forbes, A. Dudley, and M. McLaren, "Creation and detection of optical modes with spatial light modulators," Adv. Opt. Photonics **8**(2), 200–227 (2016).
11. A. D'Errico, R. D'Amelio, B. Piccirillo, F. Cardano, and L. Marrucci, "Measuring the complex orbital angular momentum spectrum and spatial mode decomposition of structured light beams," Optica **4**(11), 1350–1357 (2017).
12. K. Pang, C. Liu, G. Xie, Y. Ren, Z. Zhao, R. Zhang, Y. Cao, J. Zhao, H. Song, H. Song, L. Li, A. N. Willner, M. Tur, R. W. Boyd, and A. E. Willner, "Demonstration of a 10 Mbit/s quantum communication link by encoding data on two Laguerre-Gaussian modes with different radial indices," Opt. Lett. **43**(22), 5639–5642 (2018).
13. S. Zhu, S. Pidishety, Y. Feng, S. Hong, J. Demas, R. Sidharthan, S. Yoo, S. Ramachandran, B. Srinivasan, and J. Nilsson, "Multimode-pumped Raman amplification of a higher order mode in a large mode area fiber," Opt. Express **26**(18), 23295–23304 (2018).
14. S. Pachava, A. Dixit, and B. Srinivasan, "Modal decomposition of optical fiber output in OAM basis using optical correlation technique," in Laser Congress 2018 (ASSL), OSA Technical Digest (Optical Society of America, 2018), paper AM6A.29.
15. D. Flamm, C. Schulze, R. Brüning, O. A. Schmidt, T. Kaiser, S. Schröter, and M. Duparré, "Fast M^2 measurement for fiber beams based on modal analysis," Appl. Opt. **51**(7), 987–993 (2012).
16. A. Trichili, A. B. Salem, A. Dudley, M. Zghal, and A. Forbes, "Encoding information using Laguerre Gaussian modes over free space turbulence media," Opt. Lett. **41**(13), 3086–3089 (2016).
17. J. W. Goodman, Introduction to Fourier Optics (Roberts and Company Publishers, 2005)
18. J. A. Davis, D. M. Cottrell, J. Campos, M. J. Yzuel, and I. Moreno, "Encoding amplitude information onto phase-only filters," Appl. Opt. **38**(23), 5004–5013 (1999).
19. L. Zhu and J. Wang, "Arbitrary manipulation of spatial amplitude and phase using phase-only spatial light modulators," Sci. Rep. **4**(1), 7441 (2014).
20. V. Arrizón, U. Ruiz, R. Carrada, and L. A. González, "Pixelated phase computer holograms for the accurate encoding of scalar complex fields," J. Opt. Soc. Am. A **24**(11), 3500–3507 (2007).
21. V. Arrizón, G. Méndez, and D. Sánchez-de-La-Llave, "Accurate encoding of arbitrary complex fields with amplitude-only liquid crystal spatial light modulators," Opt. Express **13**(20), 7913–7927 (2005).
22. G. N. Watson, A Treatise on the Theory of Bessel Functions (Cambridge University, 1922).
23. J. George, R. Seihgal, S. M. Oak, and S. C. Mehendale, "Beam quality degradation of a higher order transverse mode beam due to spherical aberration of a lens," Appl. Opt. **48**(32), 6202–6206 (2009).
24. J. M. Andersen, S. N. Alperin, A. A. Voitiv, W. G. Holtzmann, J. T. Gopinath, and M. E. Siemens, "Characterizing vortex beams from a spatial light modulator with collinear phase-shifting holography," Appl. Opt. **58**(2), 404–409 (2019).
25. S. Choudhary, R. Sampson, Y. Miyamoto, O. S. Magaña-Loaiza, S. M. H. Rafsanjani, M. Mirhosseini, and R. W. Boyd, "Measurement of the radial mode spectrum of photons through a phase-retrieval method," Opt. Lett. **43**(24), 6101–6104 (2018).
26. F. Bouchard, N. H. Valencia, F. Brandt, R. Fickler, M. Huber, and M. Malik, "Measuring azimuthal and radial modes of photons," Opt. Express **26**(24), 31925–31941 (2018).
27. D. Fu, Y. Zhou, R. Qi, S. Oliver, Y. Wang, S. M. H. Rafsanjani, J. Zhao, M. Mirhosseini, Z. Shi, P. Zhang, and R. W. Boyd, "Realization of a scalable Laguerre-Gaussian mode sorter based on a robust radial mode sorter," Opt. Express **26**(25), 33057–33065 (2018).